Supporting Information

Zinc Hexacyanoferrate with Highly Reversible Open Framework for Fast Aqueous Nickel-Ion Storage

Jichen Zhao[1], Jiaxi Xu[1], Xikun Zhang[1], Yiwen Liu, Chiwei Xu, Junwei Zhang, Haoxiang Yu, Lei Yan, Jie Shu**

School of Materials Science and Chemical Engineering, Ningbo University, Ningbo, Zhejiang, 315211, China

[1] These authors contributed equally to this work.

* Corresponding author: Jie Shu

E-mail: shujie@nbu.edu.cn

* Corresponding author: Lei Yan

E-mail: yanlei@nbu.edu.cn

$$I_p = a\upsilon^b \tag{1}$$

I_p: peak current(mA), υ: scan rate (mV s^{-1}), a and b: adjustable constants.

$$I_P = k_1\upsilon + k_2\upsilon^{\frac{1}{2}} \tag{2}$$

I_p: peak current (mA), υ: scan rate (mV s^{-1}), k_1 and k_2: adjustable constants.

$$D = \frac{0.5R^2T^2}{A^2n^4F^4C^2\sigma^2} \tag{3}$$

D: diffusion coefficient, R: gas constant, T: temperature, A: electrode area, n: electrons transfer number, F: Faraday constant, C: concentration of Ni^{2+}, σ: Warburg coefficient.

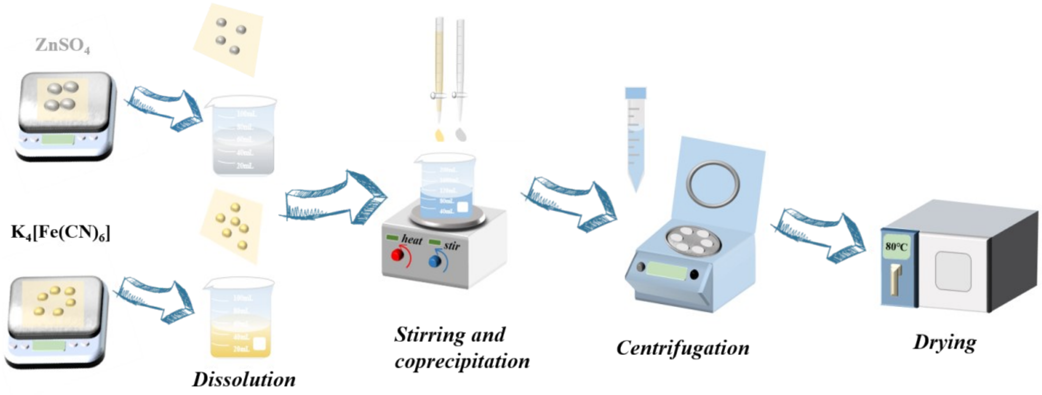

Fig. S1. Synthetic procedure of K-ZnHCF**.**

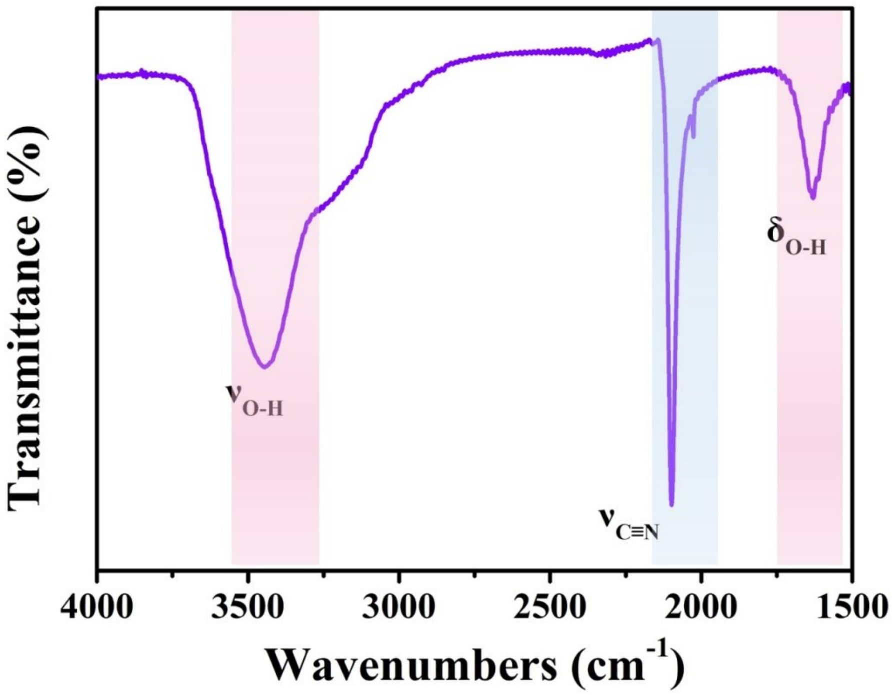

Fig. S2. FTIR spectrum of K-ZnHCF.

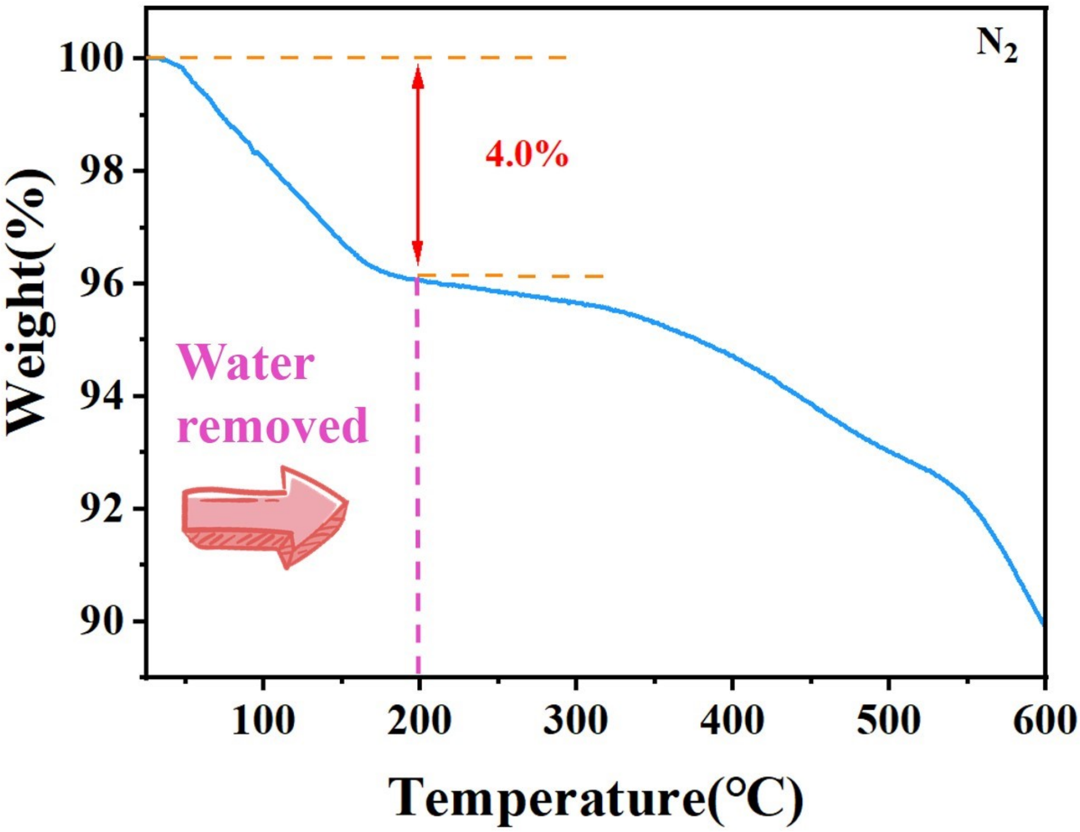

Fig. S3. TGA curve of K-ZnHCF from 25 to 600°C.

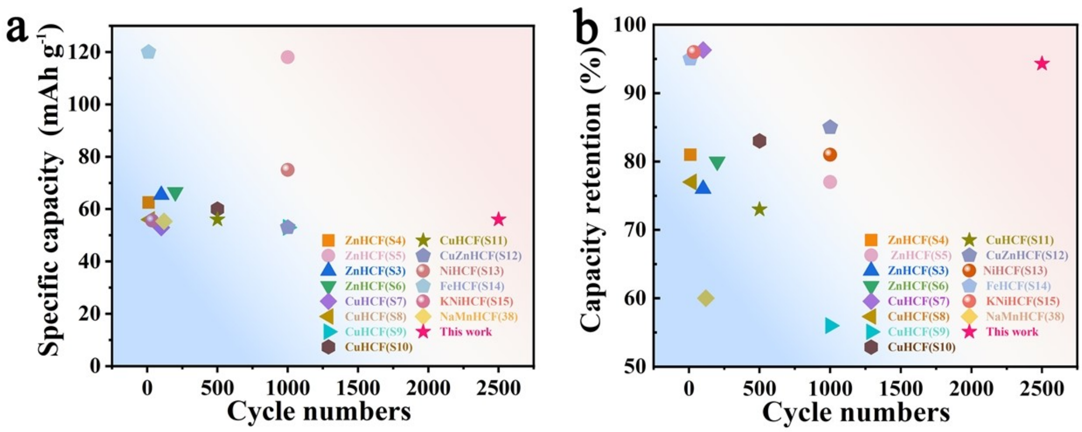

Fig. S4. Comparison of cycle performance between this work and PBAs-based zinc ions batteries. (a) Specific capacity. (b) Capacity retention.

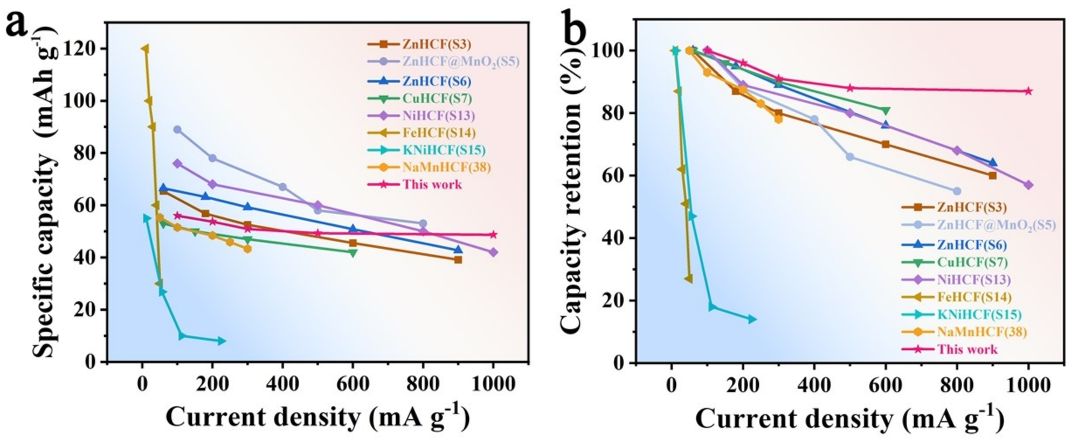

Fig. S5. Comparison of rate performance between this work and PBAs-based zinc ions batteries. (a) Specific capacity. (b) Capacity retention.

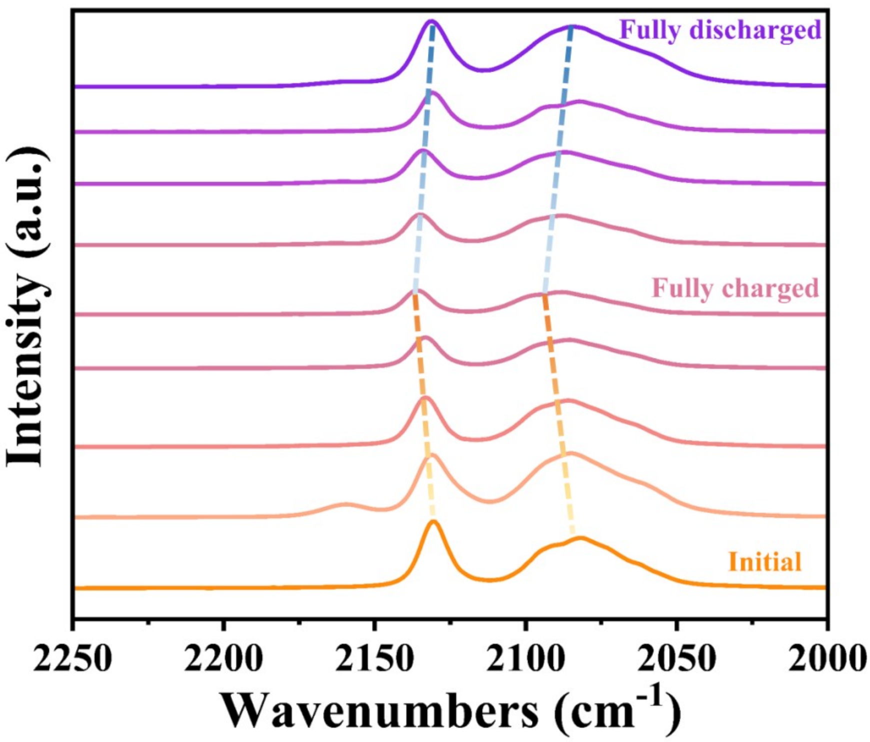

Fig. S6. Ex-situ Raman spectra of K-ZnHCF during electrochemical cycle.

Table S1. Rietveld refinement data obtained for K-ZnHCF material.

Site	Atom	x	y	z	Occupancy
a = b = 12.53676 Å, c= 32.09520 Å, R_p *= 9.77 %,* R_{wp} *= 12.3 %*					
36f	C(1)	0.14089	-0.02186	0.17739	1.00
36f	C(2)	0.54215	0.23880	0.23880	1.00
36f	N(1)	0.18763	-0.02742	0.20583	1.00
36f	N(2)	0.44938	0.14714	0.23903	1.00
12c	Fe	0.00000	0.00000	0.14821	0.333
18e	Zn	0.28703	0.00000	0.25000	0.500
36f	K	0.55863	0.35284	0.30771	0.300
36f	O(1)	0.45040	0.26570	0.31724	0.170
36f	O(2)	0.47441	0.29932	0.31775	0.150
36f	O(3)	0.51967	0.40351	0.31127	0.280
36f	O(4)	0.41772	0.36038	0.29450	0.560
36f	O(5)	0.33359	0.32381	0.27443	0.400

Table S2. The comparison of electrochemical performance between this work and recently reported aqueous batteries.

Material	Charge carrier	Reversible capacity	Voltage polarization	Cycling performance	Ref.
$Na_2Co[Fe(CN)_6]$	Na^+	150mAh g^{-1}	0.15V	90%/200/100	[S1]
$Fe_4[Fe(CN)_6]_3 \cdot 3.4H_2O$	K^+	67mAh g^{-1}	0.16V	82.4%/500/100	[33]
FeNiHCF	Na^+	106mAh g^{-1}	0.08V	96%/100/10	[S2]
$Zn_3[Fe(CN)_6]_2$	Zn^{2+}	52.5mAh g^{-1}	0.33V	81%/100/300	[S3]
K-ZnHCF	Ni^{2+}	56.2mAh g^{-1}	0.06V	96%/2500/100	This work

The cycling performance is summarized as capacity retention/cycle number/current density (mA g^{-1}).

Table S3. The comparison of electrochemical performance between this work and recently reported PBAs-based Zn ions batteries.

Materials	Electrolyte	Capacity retention (%)	Cycle numbers	Current density ($mA\cdot g^{-1}$)	Specific capacity ($mAh\ g^{-1}$)	Voltage range (V)	Ref.
ZnHCF	1 M $ZnSO_4$	76%	100	300	65.4	0.8–2.0 (*vs.* Zn^{2+}/Zn)	S3
ZnHCF	0.1 M $ZnSO_4$	81%	10	40	62.5	1.2-2.05 (*vs.* Zn^{2+}/Zn)	S4
ZnHCF@MnO_2	0.5 M $ZnSO_4$	77%	1000	500	118	1.4-1.9 (*vs.* Zn^{2+}/Zn)	S5
ZnHCF	3 M $ZnSO_4$	80%	200	300	66.5	0.8–2.0 (*vs.* Zn^{2+}/Zn)	S6
CuHCF	0.02 $ZnSO_4$	96.3%	100	60	53	0.6–1.3 (*vs.* SHE)	S7
CuHCF	1 M $ZnSO_4$	77%	20	20	56	0–1.1 (*vs.* SCE)	S8
CuHCF	0.1 M $ZnSO_4$	56%	1000	50	53	0.2–1.1 (*vs.* Ag/AgCl)	S9
CuHCF	1 M Na_2SO_4	83%	500	300	60	1.4-2.1 (vs. Zn^{2+}/Zn)	S10
CuHCF	2 M $NaClO_4$	73%	500	300	56	0.4–1.3 (*vs.* SHE)	S11
CuZnHCF	0.02 M $ZnSO_4$	85%	1000	85	53	0.2–1.1 (*vs.* Ag/AgCl)	S12

NiHCF	0.5 M Na_2SO_4 + 0.05 M $ZnSO_4$	81%	1000	500	75	0.9–1.9 (*vs.* Zn^{2+}/Zn)	S13
FeHCF	1 M $Zn(OAc)_2$	95%	10	10	120	0.8–2.0 (*vs.* Zn^{2+}/Zn)	S14
KNiHCF	0.5 M $Zn(ClO_4)_2$	96%	35	56	55.6	0.7–1.8 (*vs.* Zn^{2+}/Zn)	S15
NaMnHCF	1 M $ZnSO_4$	60%	120	50	55.3	0-1 (*vs.* Ag/AgCl)	38
K-ZnHCF	0.5 M $Ni(Ac)_2$	94.3%	2500	100	56	-0.5-0.9 (*vs.* Ag/AgCl)	This work

Reference

S1 X.Y. Wu, C.H. Wu, C.X. Wei, L. Hu, J.F. Qian, Y.L. Cao, X.P. Ai, J.L. Wang, H.X. Yang, Highly crystallized $Na_2CoFe(CN)_6$ with suppressed lattice defects as superior cathode material for sodium-ion batteries, *ACS Appl. Mater. Interfaces*. 2016, **8**, 5393-5399.

S2 S.L. Yu, Y. Li, Y.H. Lu, B. Xu, Q.T. Wang, M. Yan, Y.Z. Jiang, A promising cathode material of sodium-iron nickel hexacyanoferrate for sodium ion batteries, *J. Power Sources*, 2015, **275**, 45-49.

S3 L.Y. Zhang, L. Chen, X.F. Zhou, Z.P. Liu, Towards high-voltage aqueous metal-ion batteries beyond 1.5 V: the zinc/zinc hexacyanoferrate system, *Adv. Energy Mater.*, 2015, **5**, 1400930.

S4 B. Tang, L. Shan, S. Liang, J. Zhou, Issues and opportunities facing aqueous zinc-ion batteries, *Energy Environ. Sci.*, 2019, **12**, 3288-3304.

S5 K. Lu, B. Song, Y. Zhang, H. Ma, J. Zhang, Encapsulation of zinc hexacyanoferrate nanocubes with manganese oxide nanosheets for high-performance rechargeable zinc ion batteries, *J. Mater. Chem. A*, 2017, **5**, 23628-23633.

S6 L. Zhang, L. Chen, X. Zhou, Z. Liu, Morphology-dependent electrochemical performance of zinc hexacyanoferrate cathode for zinc-ion battery, *Sci. Rep.*, 2015, **5**, 18265.

S7 R. Trócoli, F. La Mantia, An aqueous zinc-ion battery based on copper hexacyanoferrate, *ChemSusChem*, 2015, **8**, 481-485.

S8 Z. Jia, B. Wang, Y. Wang, Copper hexacyanoferrate with a well-defined open framework as a positive electrode for aqueous zinc ion batteries, *Mater. Chem. Phys.*, 2015, **149**, 601-606.

S9 J. Lim, G. Kasiri, R. Sahu, K. Schweinar, K. Hengge, D. Raabe, F. La Mantia, C. Scheu, Irreversible structural changes of copper hexacyanoferrate used as a cathode in Zn-ion batteries, *Chem. Eur. J.,* 2019, **26**, 4917-4922.

S10 T. Gupta, A. Kim, S. Phadke, S. Biswas, T. Luong, B. J. Hertzberg, M. Chamoun, K. Evans-Lutterodt, D. A. Steingart, Improving the cycle life of a high-rate, high-potential aqueous dual-ion battery using hyper-dendritic zinc and copper hexacyanoferrate, *J. Power Sources*, 2016, **305**, 22-29.

S11 R. Trócoli, G. Kasiri, F. La Mantia, Phase transformation of copper hexacyanoferrate ($KCuFe(CN)_6$) during zinc insertion: effect of Co-ion intercalation, *J. Power Sources*, 2018, **400**, 167-171.

S12 G. Kasiri, J. Glenneberg, A. B. Hashemi, R. Kun, F. La Mantia, Mixed copper-zinc hexacyanoferrates as cathode materials for aqueous zinc-ion batteries, *Energy Storage Mater.*, 2019, **16**, 360-369.

S13 K. Lu, B. Song, J. Zhang, H. Ma, A rechargeable Na-Zn hybrid aqueous battery fabricated with nickel hexacyanoferrate and nanostructured zinc, *J. Power Sources*, 2016, **321**, 257-263.

S14 Z. Liu, G. Pulletikurthi, F. Endres, A Prussian blue/zinc secondary battery with a bio-ionic liquid-water mixture as electrolyte, *ACS Appl. Mater. Interfaces*, 2016, **8**, 12158-12164.

S15 M. S. Chae, J. W. Heo, H. H. Kwak, H. Lee, S. T. Hong, Organic electrolyte-based rechargeable zinc-ion batteries using potassium nickel hexacyanoferrate as a cathode material, *J. Power Sources*, 2017, **337**, 204-211.